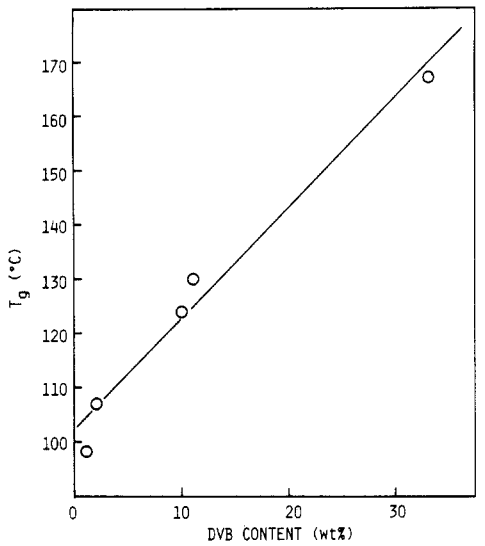

Figure 7. Relationship between T_g and DVB content of ST–DVB copolymers.

networks exhibit basically the same tendency as monotonous functions of the DVB content in the copolymers. Here, considering the polydispersity of the ST sequences between the networks, $\bar{M}_w/\bar{M}_n$ should be much greater than unity. However, the estimated $\bar{M}_w$'s from dimer and trimer yields are lower than those expected from the $\bar{M}_n$ obtained from T_g values. These discrepancies might be attributed to the following reasons: (a) The roughly estimated $\bar{M}_n$'s from T_g values contain the contribution of EST sequences to some extent depending on the composition of the copolymers. (b) The ST sequences in the networks may behave differently rather than similarly to those in linear PS's during their thermal degradation even at high temperatures around 600 °C. (c) The molecular weight distribution of the ST sequences between the networks is too wide to adopt eq 5 where the distribution range is regarded to be narrow enough.

In order to confirm these possible reasons, various ST–DVB copolymers synthesized anionically and their precursor PS's are currently under investigation by PyGC.

Acknowledgment. We are indebted to Showa-Denko Industry Inc. and Toyo-Soda Industry Inc. for providing the various ST–DVB copolymers. We also thank K. Matsumoto for GC–MS measurements and helpful discussion. Financial support in the form of a Grant-in-Aid from the Ministry of Education is gratefully acknowledged.

References and Notes

(1) Rietsch, F.; Froelich, D. *Polymer* **1975**, *16*, 873.
(2) Rietsch, F.; Daveloose, D.; Froelich, D. *Polymer* **1976**, *17*, 859.
(3) Rietsch, F.; Brault, A.; Froelich, D. *Polymer* **1978**, *19*, 1043.
(4) Brault, A.; Rietsch, F.; Froelich, D. *Polymer* **1978**, *19*, 1047.
(5) Rietsch, F. *Macromolecules* **1978**, *11*, 477.
(6) Rietsch, F.; Froelich, D. *Eur. Polym. J.* **1979**, *15*, 349.
(7) Rietsch, F.; Froelich, D. *Eur. Polym. J.* **1979**, *15*, 361.
(8) Sellier, N.; Jones, C. E. R.; Guiochon, G. In "Analytical Pyrolysis"; Jones, C. E. R., Cramers, C. A., Eds.; Elsevier: Amsterdam, 1977.
(9) Popov, G.; Haüsler, K. G.; Krauss, D.; Schuwachula, G. *Plaste Kautsch.* **1980**, *27*, 614.
(10) Sugimura, Y.; Tsuge, S. *Anal. Chem.* **1978**, *50*, 1968.
(11) Tsuge, S.; Okumoto, T.; Takeuchi, T. *J. Chromatogr. Sci.* **1969**, *7*, 250.
(12) Ohtani, H.; Tsuge, S.; Matsushita, Y.; Nagasawa, M. *Polym. J. (Tokyo)* **1982**, *14*, 495.
(13) Nielsen, L. E. *J. Macromol. Sci., Rev. Macromol. Chem.* **1969**, *3*, 69.

Heterogeneity in Branching: Mathematical Treatment of the Amylopectin Structure

Walther Burchard* and Angelika Thurn

Institute of Macromolecular Chemistry, University of Freiburg, Freiburg, FRG.
Received October 22, 1984

ABSTRACT: Heterogeneity in the branching density of amylopectin was disclosed 15 years ago by enzymatic debranching experiments. The question whether such heterogeneity has significant influence on the angular dependence of scattered light from the non-degraded molecule is examined in the present paper. On the basis of cascade branching theory, the two molecular weight averages M_w and M_n, the mean-square radius of gyration $\langle S^2 \rangle_z$, and the particle scattering factor $P_z(q)$ have been calculated for the following three models discussed in the literature: (i) the homogeneous Meyer Model, (ii) the heterogeneously branched French model, and (iii) a modified heterogeneously branched structure suggested by Robin and Mercier. The model calculations were carried out under the constraint of the same average branching density as found experimentally. This constraint, together with the experimentally observed length of branches of 22, 44, and 66 units, leads to the existence of densely branched clusters with three to four branching points on the average. Excellent agreement is obtained with the modified Robin–Mercier model, where the chains connecting the cluster carry on the average 1.4 clusters.

Introduction

Polymer science is now a highly developed field, but there still exist a few products, mainly of natural origin, for which, in spite of immense effort, the structure is not sufficiently well-known. The energy-storing biopolymers amylopectin (AP) and glycogen are typical examples. Both of these polysaccharides are highly branched, and the complexity in structure compared to linear chains is considerable.

At first sight, it might appear hopeless ever to find a satisfactory theory of the properties of branched polymers. This is, however, not true for synthetic polymers, where branching occurs essentially at random. This randomness facilitates the application of statistical methods,[1-5] and many properties of synthetic branched resins can now be described very satisfactorily[6] by the Flory–Stockmayer theory. More difficult is the treatment of a branched structure that is subject to incisive constraints[7,8] or that

0024-9297/85/2218-2072$01.50/0

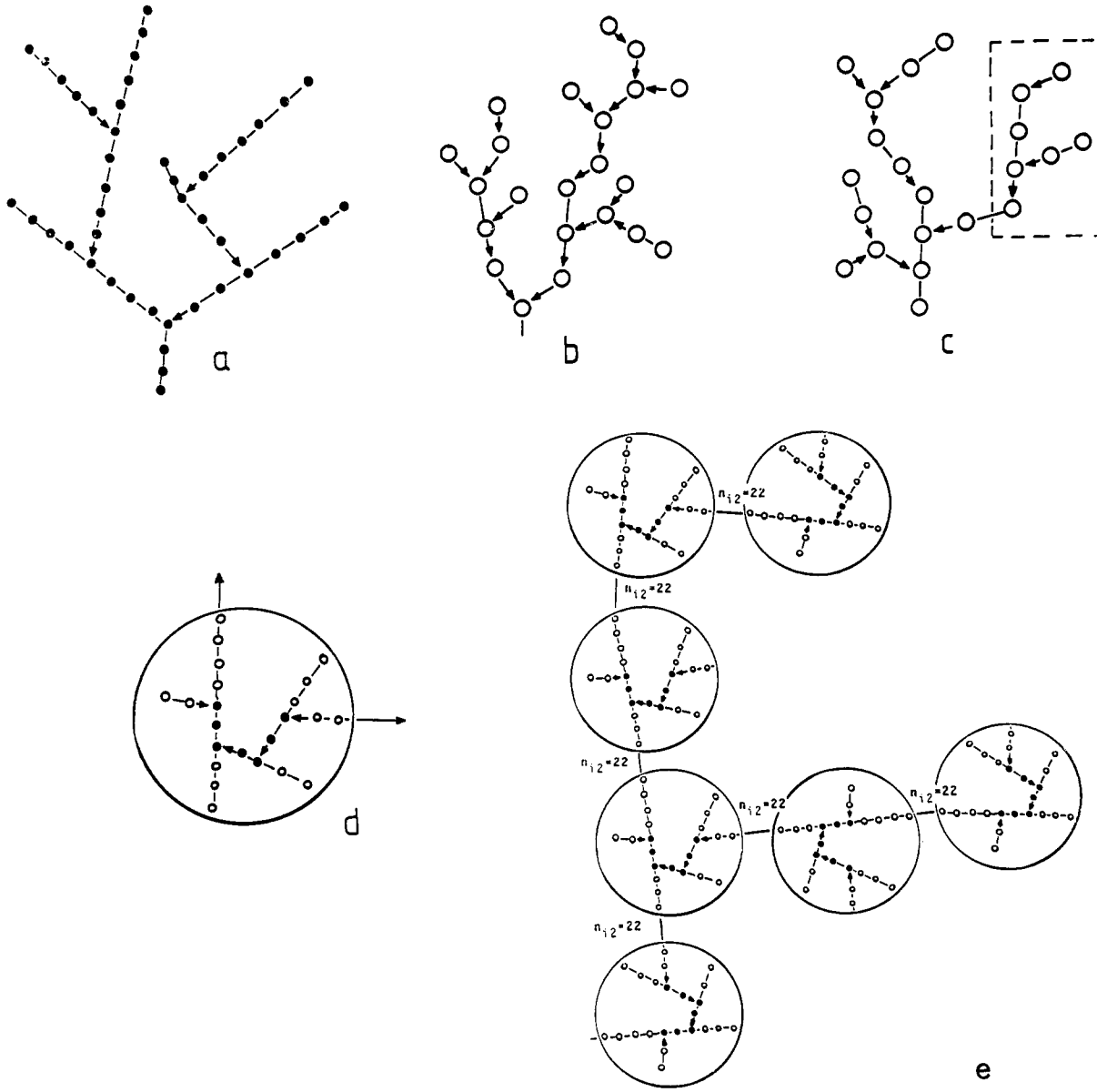

Figure 1. (a) Meyer model (homogeneous), (b) French model (heterogeneous), (c) modified Robin–Mercier model (heterogeneous). The filled circles (●) in graph a denote individual glucose units where the arrow (→) indicates α-(1,6) branching points and the edges (—) α-(1,4) glucosidic bonds. Graphs b and c are contracted graphs in which the open circles (○) no longer represent individual glucose units, but symbolize a densely branched cluster, the detailed structure of which is shown in graph d. The lines represent linear α-(1,4) chains of $\bar{n}_{i2}$ = 22 glucose units in length connecting the clusters of type d and are not individual bonds. The arrows indicate that these chains are linked by α-(1,6) bonds to cluster d. (d) represents an expanded graph of the internal clusters of (b) and (c). Here the filled circles belong to the internal structure of the cluster, while the open circles belong to the outer chains ($\bar{n}_o$ = 13.5 or 2.5 for AP and its α-LD, respectively). The arrows outside of the big circle indicate the chains connecting two clusters with the length $\bar{n}_{i2}$ = 22. The difference between (b) and (c) is demonstrated in graph e by the detailed structure of a section of the molecule as indicated by the dotted line in (c). A side chain has in this case a length $\bar{n}_{is} = \bar{n}\cdot\bar{n}_{i2} = \bar{n}\cdot 22$, where $\bar{n}$ is the average number of clusters per side chain. Note: In the original Robin–Mercier model $\bar{n}$ = 2 is *not an average value*; in the modified Robin–Mercier model $\bar{n}$ is an *average value* and was found to be $\bar{n}$ = 1.4.

is synthesized by a regularization process, as is usually the case in enzymatic reactions.

For a long time AP and glycogen were considered to be homogeneously branched. Such structures can be described by a model suggested by Meyer and Bernfeld,[9] where only the average branching density is required. Later, however, French and co-workers,[10–12] as well as Whelan and his group,[13–15] discovered that AP must be heterogeneous in its branching densities. Most convincing were the debranching experiments with the two enzymes pullulanase and isoamylase by Mercier et al.[13,16,17] French, and later Robin et al., came to suggest models in which densely branched clusters are connected via longer chains. The two models differ only in details and may be called in the following the French model (II) and the Robin–Mercier model (III) (see Figure 1).

All models suggested so far rest on the basis of enzymatic degradation experiments and the analysis of the oligomeric products obtained. Only in rare cases have the properties of the undamaged macromolecule been considered.[2,18–20] The various forms of structure must have, however, a marked influence on the solution behavior, i.e., polydispersity, overall molecular dimensions, hydrodynamic behavior, and internal mobility.

The interest of this paper is focused on the properties of the degraded native structure of AP, which can be determined by light scattering (LS) and hydrodynamic techniques.[21] We have carried out statistical model calculations for the angular dependence of the scattered light in which the special details of the various proposed models

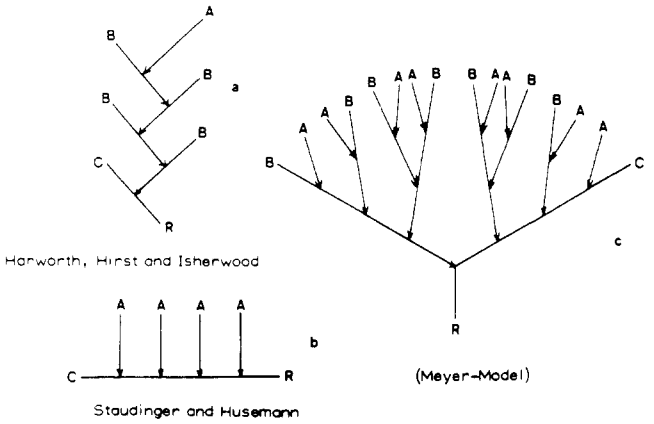

Figure 2. Branching structure for amylopectin according to (a) Harworth, Hirst, and Isherwood[25] (laminar structure), (b) Staudinger and Husemann[24] (comblike structure), and (c) Meyer and Bernfeld[9] (tree-type structure). Only model c gives the correct ratio $A:B = 1$. C is the only B chain in the molecule with the reducing end group R. An A chain is always an unbranched outer chain. B chains are always branched, but parts of them also form outer chains.

have been taken into consideration. The purpose of these calculations is to examine whether the difference in the models produces a significant change in the particle scattering factor that may allow confirmation of one of these models and the exclusion of the two others.

In order to avoid distracting mathematical details, this paper is divided into two parts. In the first, we present the particularities of the different models; we briefly discuss the principles of the calculation and present results. In the second (Appendix), details of the mathematical treatment are given.

Topological Relationships of Branched Chains

All mooels have to fulfill two special requirements; (i) The ratio of the number (A) of outer (A) chains and the number (B) of inner chains (B) has to be 1, as has been found in most nattive amylopectins and glycogens.[22,23] (ii) The branching density derived from the models must agree with the experimental value.

The following consideration will be confined to trifunctional branching units. The difference between A and B chains may be demonstrated with the homogeneously branched Meyer Model (Figure 2). An A chain is in every case an outer chain, i.e., linked by an α-(1,6)-glycosidic bond to another chain. A B chain, on the other hand, bears at least one or more branching points. Thus, not all outer chains are A chains, but the outermost section of a B chain is also an outer chain, where the linkage at the branching point is now an α-(1,4)-glycosidic bond.

The ratio of A to B chains is characteristically different in various structures. A comblike molecule[24] has one B chain only; the others are A chains, so $A:B$ goes to infinity with increasing molecular weight. In the laminar structure, suggested by Harworth, Hirst, and Isherwood,[25] the opposite behavior is found, i.e., $A:B \rightarrow 0$. The Meyer model gives just the correct ratio of $A:B = 1$[23] (Figure 2).

Next, the average branching density has to be defined. This quantity may be explained first with the homogeneously branched Meyer model and second with the exammple of the French model.

Homogeneous Branching. Let K be the number of branching points per macromolecule, and $\bar{n}_o$ and $\bar{n}_i$ the average chain length of the outer and inner chains (see Figure 4); the branching density, DB, is defined as the number of branching points, K, per molecule (i.e., per P_n). The number-average degree of polymerization, P_n, can be

Table I
Branching Density DB and the Resulting Inner and Outer Average Chain Length $\bar{n}_i$ and $\bar{n}_o$ for AP and Its β-LD

	AP	β-LD
$DB^{-1} = \bar{n}_i + \bar{n}_o$	25	14
$\bar{n}_i$	11.5	11.5
$\bar{n}_o$	13.5	2.5

calculated from the number of branching points, K, and the average length of the inner and outer chains, and is given by

$$P_n = \bar{n}_o(K + 1) + \bar{n}_1(K - 1) + \bar{n}_r \quad (1a)$$

which for $K \gg 1$ becomes

$$P_n \rightarrow K(\bar{n}_i + \bar{n}_o) \quad (1b)$$

Here $\bar{n}_r$ is the only outer chain with a reducing end group. With eq 1 one finds the branching density DB

$$DB = K/P_n = 1/[(\bar{n}_i + \bar{n}_o) + (\bar{n}_o - \bar{n}_i + \bar{n}_r)/K] \rightarrow 1/(\bar{n}_i + \bar{n}_o) \quad (2)$$

Thus for large molecules the branching density defines the sum of one inner and one outer chain. The branching density can be measured directly and is the ratio of branching points to the number of repeating units in the system.

Equations 1 and 2 hold for both homogeneously and heterogeneously branched molecules and are valid for AP as well as for its β-limit dextrin (β-LD). In the latter case, $\bar{n}_o = 2.5$, which is known from the mechanism of β-amylase action.[26] According to eq 2 only the *sum* of an inner and outer chain can be calculated from the degree of branching. In order to determine $\bar{n}_i$ and $\bar{n}_o$ separately one has to measure the fraction X of the mass of β-LD and AP used before β-amylase digestion

$$X = (\text{mass})_{\beta\text{-LD}}/(\text{mass})_{AP} = P_{n\beta\text{-LD}}/P_{nAP} \quad (3)$$

where the second equivalence is a generally accepted approximation.[27] Making use of eq 1 and 2 one finds

$$X = (\bar{n}_i + 2.5)/(\bar{n}_i + \bar{n}_o) \quad (4a)$$

or

$$X = DB(\bar{n}_i + 2.5) \quad (4b)$$

$$\bar{n}_i = (X/DB) - 2.5 \quad (5a)$$

$$\bar{n}_o = (1/DB) - \bar{n}_i \quad (5b)$$

The density of branching varies[28] for the different AP's from $DB = 0.036$ to 0.045, and a fraction $X = 0.53$–0.56 is usually found. In the following calculations we use values of $DB = 0.04$ and $X = 0.56$. Then for AP and its β-LD the values of Table I are obtained.

Heterogeneous Branching. The relationships of eq 1–5 are general and hold also for heterogeneously branched AP's. However, $\bar{n}_i$ is now the average over two types of inner chain lengths. Let $\bar{n}_{ic}$ be the average inner chain length in a cluster and $\bar{n}_{i2}$ the length of chains connecting two clusters; furthermore, the number of branching points Z_k in a cluster may be introduced and also the average number of chains originating in one cluster leading to another cluster, i.e., the average number $\bar{f}$ of chains connecting two clusters. Then (see Figure 3)

$$\bar{n}_i = (\bar{f}\bar{n}_{i2} + (Z_k - 1)\bar{n}_{ic})/(Z_k + \bar{f} - 1) \quad (6)$$

or

$$Z_k = (\bar{f}\bar{n}_{i2} - (\bar{f} - 1)\bar{n}_i - \bar{n}_{ic})/(\bar{n}_i - \bar{n}_{ic}) \quad (7a)$$

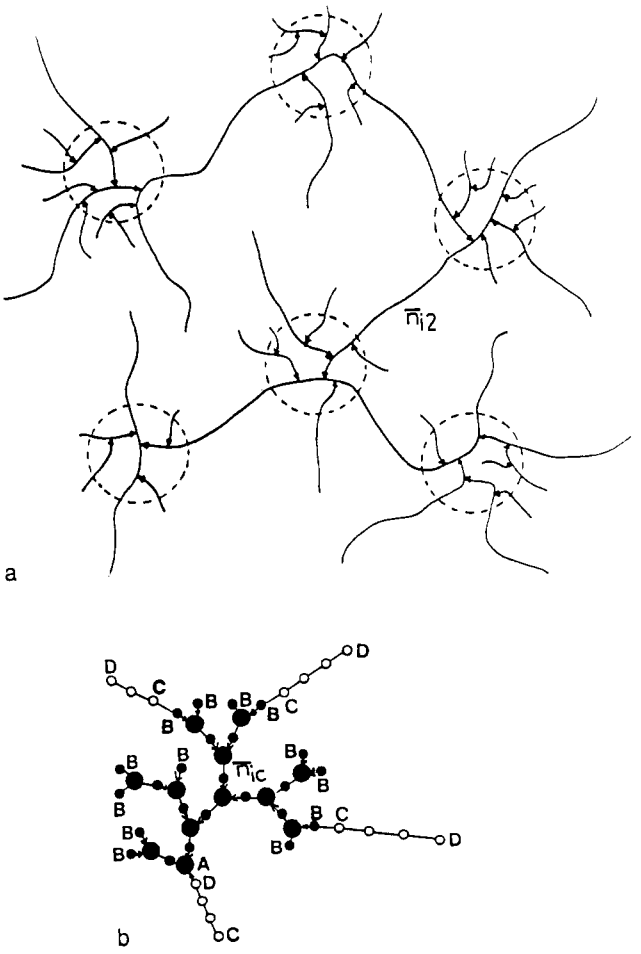

Figure 3. (a) Model of a heterogeneously branched macromolecule and (b) detail of cluster structure. C—D, interconnecting chains of the length $\bar{n}_{i2}$; ●, the Z_k branching points in a cluster.

Table II
Number of Branching Points Z_k in a Cluster Calculated for a Chain Length $\bar{n}_{i2}$ = 22 (Connecting Two Clusters) and Various $\bar{n}_{ic}$ (Inner Chains in a Cluster)[a]

	Z_k		
	n_{ic} = 2	n_{ic} = 3	n_{ic} = 4
n_{i2} = 22	3.22	3.59	3.97

[a] Total number of chains per cluster is $Z_k + 1$.

From the general theory of branching, gelation takes place when

$$(\bar{f} - 1) = 1 \tag{8}$$

which is Flory's gel condition.[3,29] Gelation does not occur in AP, though the weight-average molecular weight is very high. Thus $\bar{f}$ is very close to 2 and eq 7a reduces to

$$Z_k = (2\bar{n}_{i2} - \bar{n}_i - \bar{n}_{ic})/(\bar{n}_i - \bar{n}_{ic}) \tag{7b}$$

From the three quantities on the right-hand side of eq 7b, $\bar{n}_i$ = 11.5 was already given in eq 6 and $\bar{n}_{i2}$ was determined by Robin et al. and in our own debranching experiments[21,36] to have values in the range $\bar{n}_i$ = 20–25. The chain length $\bar{n}_{ic}$ in a cluster is unknown to date; it may range from 2 to 4. Table II gives a list of the number of branching points in a cluster for $\bar{n}_{ic}$ = 2, 3 and 4 and a length of $\bar{n}_{i2}$ = 22. The number of chains in a cluster of the type in Figure 3 is[37] $Z_k + 1$. This gives, for $\bar{n}_{i2}$ = 22 and $\bar{n}_{ic}$ = 2, on the average 4.22 chains per cluster, which is close to the suggested value of Robin et al.[16,17] These authors give in their original paper a value of 8–9, which, however, is the average number of chains for *two* clusters, since in their model one interconnecting chain always carries two clusters.

In all further calculations we assumed the highest possible branching density of 50% for the clusters,[38] i.e., $\bar{n}_{ic}$ = 2.

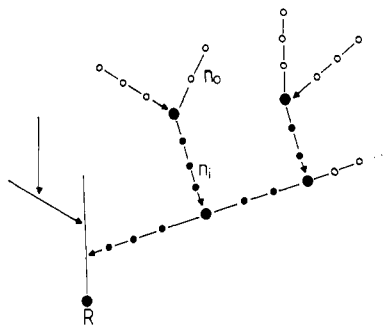

Figure 4. Schematic structure of the modified Meyer model. The internal structure corresponds to the original Meyer model, which can be generated by ABC polycondensation.[18] ● represents a trifunctional branching unit. The outer chains (–O–O–) have a degree of polymerization $\bar{n}_o$ = 13.5 for the AP, or $\bar{n}_o$ = 2.5 for the β-LD, respectively. The inner chain length (–•–•–) $\bar{n}$ = 11.5 is the average length between two branching points; → denotes an α-(1,6)-glycosidic bond.

Table III
Calculated and Experimental Values for M_w, M_n, $\langle S^2\rangle_z$, M_w/M_n, and Effective Bond Length, b, for the β-LD of the Indicated Models

		calcd		
	exptl	Meyer	French	Robin–Mercier
M_w	3.33×10^8	3.33×10^8	3.33×10^8	3.33×10^8
$(\langle S^2\rangle_z)^{1/2}$	260 nm			
M_n		8.22×10^5	9.22×10^4	3.89×10^4
M_w/M_n		4.05×10^2	3.61×10^3	8.56×10^3
b		4.36 nm	2.41 nm	0.79 nm

Models

General Remarks on the Proposed Models. The main difficulty is how to incoporate heterogeneity in branching under the constraint of $A:B$ = 1. The homogeneous Meyer model automatically meets this condition. Thus a natural extension of the Meyer model involves the choice of clusters that have the same internal structure but are smaller inn size. The ratio $A:B$ = 1 is not altered if these clusters are interconnected by longer B chains.

Meyer Model. There is no practical need for a statistical calculation for this homogeneously branched model, since the enzymatic degradation experiments have given very strong evidence of the heterogeneity of branching. Nevertheless, calculation for this model is useful, since it can serve as a substructure for the heterogeneously branched models.

Furthermore, we wish to develop a model that holds for both the AP and its β-LD, and where only the average length of the outer chains has to be changed. This is accomplished by considering a Meyer model, which is followed by coupling a branching unit with certainty (γ = 1; see Appendix) onto the end of the outer chains (modified Meyer model). This branching unit carries two other outer chains (see Figure 4). The original Meyer model was evaluated many years ago by one of the present authors[18] on the basis of the cascade branching theory, using the idea of the polycondensation of ABC-type monomers. The principles of calculating M_w and M_n, radius of gyration $\langle S^2\rangle_z$, and particle scattering factor $P_z(q)$ have been outlined previously. Further details are given in the Appendix.

The reciprocal particle scattering factor $(1/P_z)$ as a

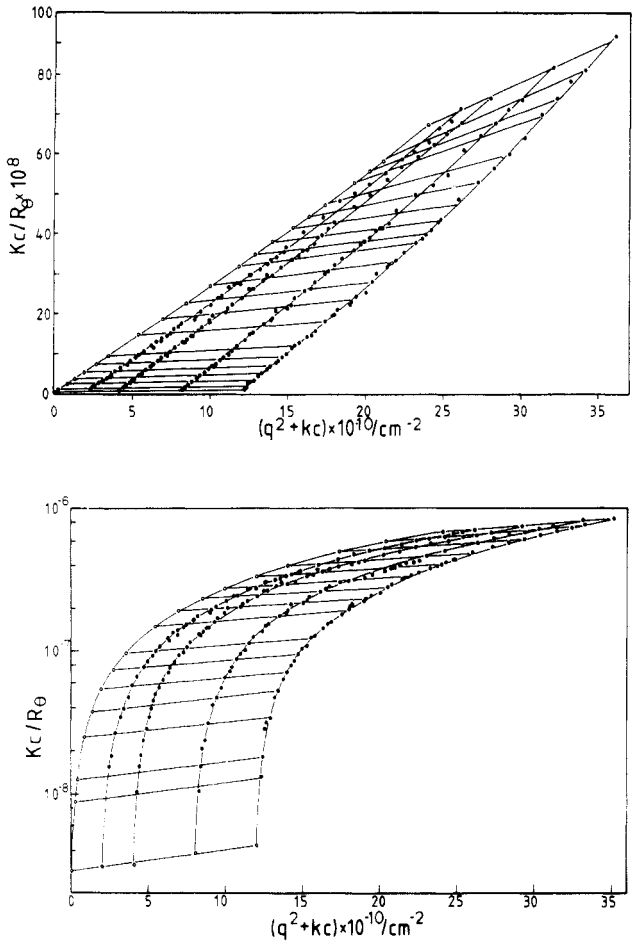

Figure 5. (a, top) Zimm plot of an amylopectin β-limit dextrin from amioca maize from light scattering measurements in 1 N NaOH. The measurements were carried out with three wave lengths, i.e., λ_0 = 546 nm (green), 436 nm (blue), and 365 nm (near UV); $q = (4\pi/\lambda) \sin(\theta/2)$, where $\lambda = \lambda_0/n_0$. Logarithmic version of the same Zimm plot (a); in this plot M_w can be determined fairly accurately. $M_w = 333 \times 10^6$, $\langle s^2 \rangle_z = 260$ nm.[19,36]

function of $u^2 = q^2\langle S^2 \rangle_z$ is shown by the pair of curves a in Figure 6. The dashed line corresponds to AP and the full line to β-LD. The particle scattering factor represents the angular dependence of the scattered light that is normalized at zero angle to $P(q = 0) = 1$; $q = (4\pi/\lambda) \sin(\theta/2)$ is the value of the scattering vector, with λ the wavelength in the medium and θ the scattering angle. The variable on the abscissa is taken as $u^2 = \langle S^2 \rangle q^2$, since then all particle scattering factors, independent of model, start with the same initial slope of $^1/_3$. The calculated curves show a strong upturn and disagree considerably with experiment (Figure 5),[18,19] as could have been anticipated from the enzymatic debranching results. In addition the molecular weight averages M_w and M_n, the mean-square radius of gyration, $\langle S^2 \rangle_z$, and the effective bond length, b, have been calculated. Table III gives the data for M_w/M_n and b for a β-LD with $M_w = 333 \times 10^6$.

French Model. As already outlined, in the French model the clusters, having the internal structure of the Meyer model, are linked via chains of length $\bar{n}_{i2} = 22$. For the branching density in the clusters we assumed DB = 0.5 (i.e., $\bar{n}_{ic} = 2$), which is the highest possible branching density.[38,40] This implies 4.22 chains per cluster on the average. These data are sufficient for a unique description of the cluster structure (e.g., M_{wc}, M_{nc}). On each of the $Z_k - 1$ chains (the cluster has all together $Z_k + 1$ outer chains, but two of them are on average chains interconnecting two clusters; therefore, the number of free outer

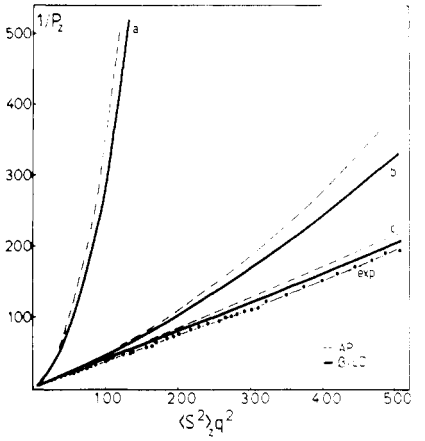

Figure 6. Reciprocal particle scattering factor, $1/P_z$, as a function of $u^2 = \langle s^2 \rangle_z q^2$ for the three models given in Figure 1 compared with $1/P_z$ measured by static LS. The dashed lines correspond to AP, the heavy lines to the β-LD; (-•-•-) experimental curve.[19,36]

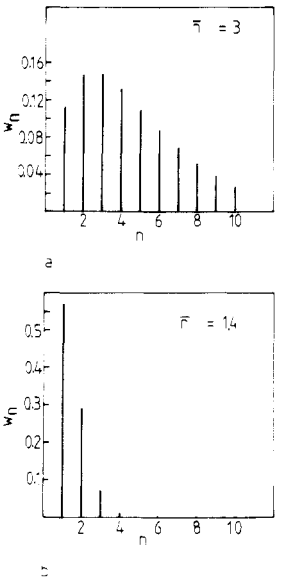

Figure 7. Calculated weight distribution of chain lengths for two different values of $\bar{n}$ (both of which give best agreement with the experimental scattering curve), and the same values of M_w/M_n. Each of the lines in this histogram represents mean values of the chain length $\bar{n}_{is} = \bar{n} \cdot \bar{n}_{i2}$, where $\bar{n}_{i2}$ is itself a distribution. A most probable distribution has been assumed.

chains is $Z_k - 1$) a linear chain of length $\bar{n}_o$ (i.e., 11.5 for AP and 2.5 for β-LD) is coupled statistically with probability $r = 1/(Z_k + 1)$. (See Appendix for details.) These modified clusters are then innerconnected by linear chains of length[39] $\bar{n}_{i2} = 22$. This is achieved by coupling both ends of the linear chain onto the remaining two free end groups of the cluster[30] (see Figure 12).

The resulting data are given in Table III, and $1/P_z$ is again plotted in Figure 6 (pair of curves b). The agreement with experiment is better, but not perfect.

Modified Robin–Mercier Model. Perfect agreement was not expected in the previous case, since our own debranching experiments[36] gave linear α-(1,4)-glycosidic linked chains with a degree of polymerization up to 75–90. We thus modified the French model, assuming linear chains that on the average carry $\bar{n}$ clusters, i.e., $\bar{n}_{is} = \bar{n} \times \bar{n}_{i2} = \bar{n} \times 22$ (see Figure 1e). All other assumptions remain the same as used for the French model with the exception that the probability of cluster interconnection has to be reduced to avoid gelation. This model differs from the suggestion by Robin et al. in two ways: (i) These authors assumed for the interconnecting chains a length of *exactly*

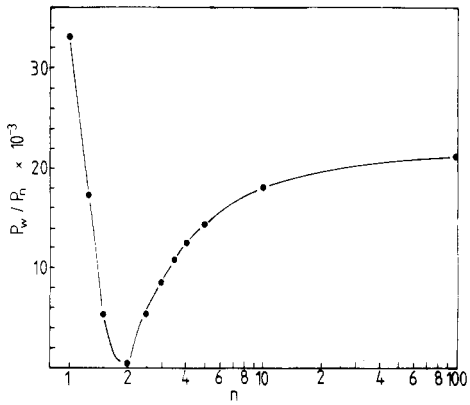

Figure 8. Calculated polydispersities P_w/P_n as function of $\bar{n}$ (defined in Figure 7) for the modified Robin–Mercier model. The model calculations allows two equivalent solutions of $\bar{n}$.

Table IV
List of Various Link Probabilities for the Modified Meyer Model Which Can Be Read from the Graph of Figure 4

	linked unit						
	l_o		b_o		b_i		
starting unit	A	B	C	D	K	L	M
A	0	α	0	$(1-\alpha)$	0	0	0
B	β	0	0	0	0	0	0
C	0	0	0	0	0	$\gamma/2$	$\gamma/2$
D	δ	0	0	0	0	0	0
K	0	0	0	0	0	λ	μ
L	0	0	$(1-\lambda)$	0	λ	0	0
M	0	0	0	0	μ	0	0

$2\bar{n}_{i2}$, while in our model the number of coupled chains $\bar{n}$ was changed systematically. (ii) This number $\bar{n}$ is in the present model an *average* value, i.e., there may be shorter and also longer chains effective in the cross-linking. The size distribution is simulated by a linear polycondensation of chains of the length $\bar{n}_{i2}$. The difference between the original Robin–Mercier model and our modification is schematically shown in Figure 7 for two values of $\bar{n}$.

Table III gives the corresponding molecular data, and the pair of curves c in Figure 6 shows the angular dependence of $1/P_z$. Almost perfect agreement with experiment is now obtained for two values of $\bar{n}$, i.e., $\bar{n} = 1.4$ and $\bar{n} = 3$.

Discussion

In all of these model calculations, excluded volume effects have been neglected because of the lack of a suitable theory for branched molecules with a complex architecture. Consideration of excluded volume would probably lead to slightly altered curves. The excellent agreement of the calculated curves with the experimental angular dependence and the fact that all relevant parameters were not fitted, but were taken from degradation experiments, gives strong evidence for the validity of the modified Robin–Mercier model. There remains the uncertainty that the

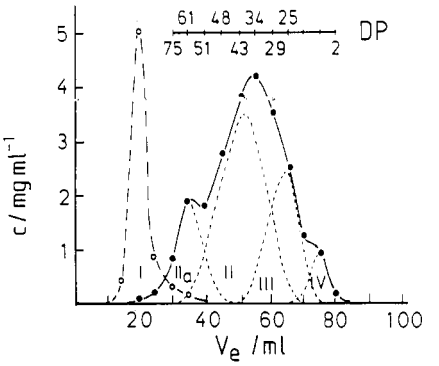

Figure 9. GPC elution diagram of debranched β-LD.[36] Four peaks referring to different linear chain length can be identified: peak IV, Stubs of outer chains $\bar{n}_o = 2$–7 (not completely resolved); peak III, $\bar{n}_{i2} = 22$; peak II, $\bar{n}_{i2} = \cong 2 \cdot 22 \cong 44$; peak IIa, $\bar{n}_{i2} = \cong 3 \cdot 22 \cong 66$. Peak I, elution diagram of the nondebranched β-LD. Debranching was performed with pullulanase, and the oligomers were fractionated on bio rad P10 gel. DP denotes degree of polymerization.

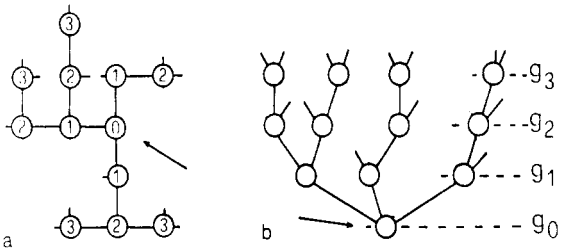

Figure 10. Structure of a trifunctional branched molecule (a) in the shell-like and (b) in a rooted tree representation. The units in the first, second, third, etc. shell of neighbors come to lie well-defined in generation g_1, g_2, g_3, etc.

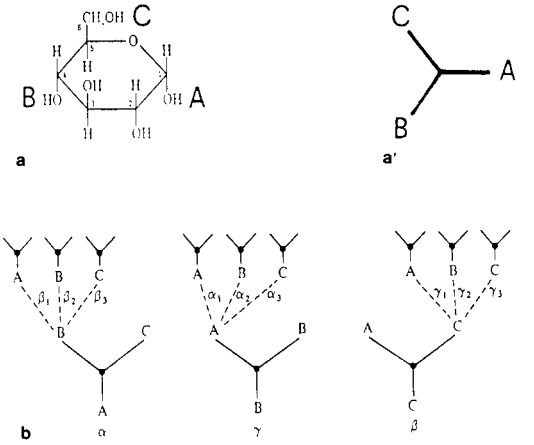

Figure 11. (a) The monomeric unit of AP is glucose, which may for simplicity be contracted to the graph a'. In AP group A be linked only to group B or C; all other reactions are excluded. (b) The various reaction probabilities for the functional groups A, B, and C of a monomeric unit in the nth generation, when group A, or B, or C is linked to a unit in the previous generation. The Greek letters denote the various link probabilities.[5]

Table V
List of Link Probabilities for the French Model according to Figure 3

	linked unit						
starting unit	A_1	B_1	A_2	B_2	C	D	E
A_1	0	α_1	0	0	0	$(1-\alpha)/2$	$1-\alpha$
B_1	β_1	0	0	0	$(1-\beta)\varkappa$	0	0
A_2	0	0	0	α_2	0	0	0
B_2	0	0	β_2	0	0	0	0
C	0	$(1-\gamma)\varkappa$	0	0	0	$(1-p)\varkappa$	$p\varkappa$
D	$r(1-\delta)$	0	$(1-r)(1-\delta)$	0	δ	0	0
E	$r(1-\epsilon)$	0	$(1-r)(1-\epsilon)$	0	ϵ	0	0

Table VI
List of Link Probabilities for the Modified Robin-Mercier Model according to Figure 4

	linked unit									
starting unit	A_1	B_1	A_2	B_2	C	D	E	R	S	T
A_1	0	α_1	0	0	0	$(1-\alpha_1)/4$	$(1-\alpha_1)/2$	0	$(1-\alpha_1)/2$	0
B_1	β_1	0	0	0	0	0	0	$1-\beta_1$	0	0
A_2	0	0	0	α_2	0	$(1-\alpha_2)/2$	$(1-\alpha_2)/2$	0	0	0
B_2	0	0	β_2	0	0	0	0	0	0	0
C	0	0	0	0	0	δ	ϵ	0	0	$\varkappa(1-\delta)$
D	$(1-\delta)r/2$	0	$(1-\delta)(1-r)/2$	0	δ	0	0	0	0	0
E	$(1-\epsilon)r/2$	0	$(1-\epsilon)(1-r)/2$	0	ϵ	0	0	0	0	0
R	0	1	0	0	0	0	0	0	0	0
S	σ	0	0	0	0	0	0	0	0	0
T	0	0	0	0	τ	0	0	0	0	0

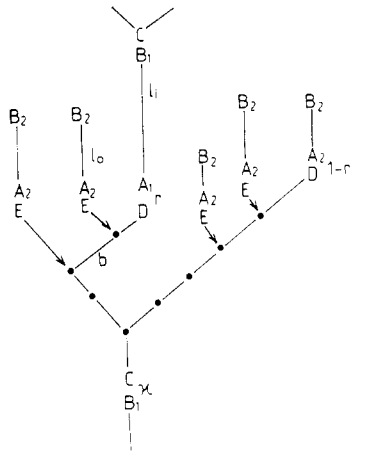

Figure 12. Rooted tree representation of the French model. The letters l_i, l_o, and b denote units from the inner chains, the outer chains, and the branched cluster. (*b* has the similar meaning as b_i in the modified Meyer model, but the branching density in the modified Meyer model is less than in the present case.) D and E groups are nonreducing end groups, i.e., OH groups in position C4 and C6, respectively, while C is a reducing end group (OH group in position C1 of the glucose).

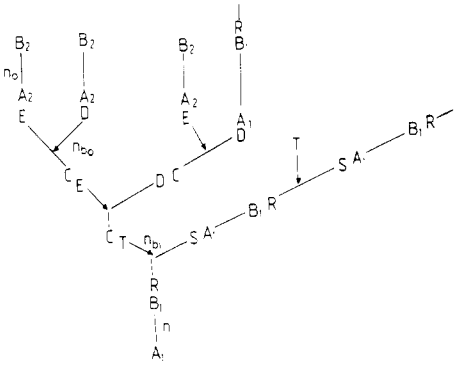

Figure 13. Rooted tree representation of the modified Robin–Mercier model. n_o, n_i, n_b, and n_{b_i} denote the mole fractions of units in the outer chain, the inner chain (connecting clusters), the cluster, and a coupling unit, respectively.

model allows two equivalent solutions for $\bar{n}$ (the only adjustable parameter), which is demonstrated in Figure 8 with the polydispersity parameter. Thus, from pure model calculations we are not able to distinguish between $\bar{n} = 1.4$ and $\bar{n} = 3$. Comparison of the GPC curves of Figure 9[36] with the calculated distributions of Figure 7, however, gives strong evidence for an average number of coupled chains of $\bar{n} = 1.4$.

It is interesting to examine the reason for the strong differences in the particle scattering factor. In previous work it has been shown[5,31,32] that regular branching causes an upturn, while polydispersity results in a downturn of these curves. Regular molecules are by definition monodisperse, while by random branching high polydispersities are produced.[3] In the latter the upturn due to branching becomes just balanced by the effect of polydispersity,[31] and a straight line is obtained.

Accordingly, the homogeneous Meyer model should exhibit the lowest polydispersity, while with the introduction of structural heterogeneity broader M_w distributions are created. Comparison of the polydispersities found for the different models show indeed an increase of polydispersity from curves a to c. This point is of some relevance, since the question has often been discussed as to whether the interconnecting linear chains are monodisperse in length. From the arguments given here, monodispersity of the chain length can be excluded, since such structures would cause a stronger upturn in $1/P_z$ than found experimentally, although a distribution slightly narrower than the assumed "most probable" length distribution may be compatible with the experimental findings.

Acknowledgment. We thank the Deutsche Forschungsgemeinschaft for financial support. We are grateful to David Brant, who carefully checked the equations in the Appendix and made valuable suggestions.

Appendix

General Remarks. In this part some details of the model calculations are given. The calculations were carried out on the basis of the cascade branching theory.[4,33,34] The mathematics is essentially a first-order Markovian chain process. For the derivation of the weight-average degree of polymerization two main quantities are needed.[5]

(I) The first one is the number of monomer units ($\langle N(1)\rangle$), which are linked to units selected at random. This number will be called the average population of units in the first shell, or in the first generation, if the molecule is represented as a rooted tree (see Figure 10).

(II) The second quantity is a set of transition probabilities, which indicate how many units in the *n*th shell are linked on the average to a unit of the preceding shell.

The calculation procedure may be demonstrated with the example of the trifunctional ABC polycondensation, which is the basis of the homogeneous Meyer model (see Figure 11), and later on with the modified Meyer model, which actually is a copolymeric model.

Model Calculations: Homogeneous Meyer Model. The monomers have to obey the constraints[18] that functionality A (reducing group at C1 in an anhydroglucose residue) can react only with group B (C4) or C (C6) (Figure 11). The extent of reaction of the three groups may be α, β, and γ; one has

$$\alpha = \beta + \gamma \tag{A1a}$$

$$\beta = (1-p)\alpha \tag{A1b}$$

$$\gamma = p\alpha \tag{A1c}$$

where p is the branching probability. From Figure 11 one directly derives

$$\langle N(1)\rangle = \alpha + \beta + \gamma = 2\alpha \tag{A2a}$$

For the following it is helpful to pass to a vector/matrix formalism,[5,33] i.e., to introduce a population vector

$$\langle \mathbf{N}(1)\rangle = (N(1)_A, N(1)_B, N(1)_C) \tag{A2b}$$

where the components denote the average number of units that are linked with their respect functional groups A, B, or C to the units which form the root of the tree (or the center in the shell-like representation). The total population is then obtained by a scalar product of a vector, $\mathbf{1} = (1,1,1)$, where all components are unity.

$$\langle N(1)\rangle = (\langle \mathbf{N}(1)\rangle \cdot \mathbf{1}) \tag{A2c}$$

To reach the next generation in the tree, one has to take into consideration whether the starting unit belongs to $N(1)_A$, or $N(1)_B$, or $N(1)_C$. For the three types of monomer units the transition probabilities can be found by inspection of Figure 11.

The total set of *transition* probabilities can be expressed by the transition-probability matrix

$$P = \begin{array}{c} \\ n-1 \\ \mathrm{A} \\ \mathrm{B} \\ \mathrm{C} \end{array} \begin{array}{c} \begin{array}{ccc} & n+1 & \\ \mathrm{A} & \mathrm{B} & \mathrm{C} \end{array} \\ \begin{pmatrix} \beta+\gamma & 0 & 0 \\ \gamma & \beta & \gamma \\ \beta & \beta & \gamma \end{pmatrix} \end{array} \tag{A3a}$$

or, with the relationships of eq A1, by

$$P = \begin{pmatrix} \alpha & 0 & 0 \\ \alpha p & (1-p)\alpha & p\alpha \\ (1-p)\alpha & (1-p)\alpha & p\alpha \end{pmatrix} \tag{A3b}$$

The vertically arranged letters A, B, and C in eq A3a indicate the types of monomer units, which are linked with their extents of reaction α, β, or γ to the preceding generation $(n-1)$. Correspondingly the three capital letters in the horizontal line indicate the functional groups of the units in the next generation $(n+1)$. The population vector in the second generation is then given by

$$\langle \mathbf{N}(2)\rangle = (\langle \mathbf{N}(1)\rangle \cdot \boldsymbol{P}) \tag{A4}$$

For all further generations the situation is the same as for the transition from the first to the second generation. Thus,

$$\langle \mathbf{N}(n)\rangle = (\langle \mathbf{N}(n-1)\rangle \cdot \boldsymbol{P}) \tag{A5}$$

and finally by performing the recursion one obtains for the population vector in the nth generation

$$\langle \mathbf{N}(n)\rangle = (\langle \mathbf{N}(1)\rangle \cdot \boldsymbol{P}_n^{n-1}) \tag{A6a}$$

and for the total population

$$\langle N(n)\rangle = [\langle \mathbf{N}(1)\rangle \cdot \boldsymbol{P}^{n-1}\mathbf{1}] \tag{A6b}$$

The weight-average degree of polymerization is obtained by summing over all generations, where $\langle N(0)\rangle = 1$. This yields

$$P_w = 1 + \sum_{N=1}^{\infty} \langle \mathbf{N}(1)\rangle \cdot \boldsymbol{P}^{n-1}\mathbf{1}$$

$$P_w = 1 + [\langle \mathbf{N}(1)\rangle \cdot (\boldsymbol{I} - \boldsymbol{P})^{-1} \cdot \mathbf{1}] \tag{A7}$$

The number-average degree of polymerization can be calculated according to a general formula given by Stockmayer.[1] This formula can be transformed into a vector/matrix notation,[5,33] which yields

$$P_n = 1/(1 - \tfrac{1}{2}[\langle \boldsymbol{N}(1)\rangle \cdot \mathbf{1}]) \tag{A8}$$

A corresponding equation for the particle scattering factor is given by the relationship

$$P_w P_z(q) = [\langle \boldsymbol{N}(1)\rangle \cdot \tilde{\phi}(\boldsymbol{I} - \boldsymbol{P}\tilde{\phi})^{-1} \cdot \mathbf{1}] \tag{A9}$$

where $\tilde{\phi}$ is a diagonal matrix with elements

$$\phi = \exp(-b^2q^2/6) \tag{A10}$$

with b the effective bond length and $q = (4\pi/\lambda)\sin(\Theta/2)$. The mean-square radius of gyration is obtained from a series expansion of the particle scattering factor

$$P_z(q) = 1 - \tfrac{1}{3}\langle S^2\rangle_z q^2 + \ldots \tag{A11}$$

or

$$\langle S^2\rangle_z = 3(\mathrm{d}P_z(q)/\mathrm{d}q^2)|_{q\to 0} \tag{A12}$$

Applying eq A12 to the relationship of eq A9 one obtains

$$\langle S^2\rangle_z = (b^2/2P_w)[\langle \mathbf{N}(1)\rangle \cdot (\boldsymbol{I} - \boldsymbol{P})^{-2} \cdot \mathbf{1}] \tag{A13}$$

Modified Meyer Model. As mentioned in the introduction, the modified Meyer model is obtained by statistical coupling of trifunctional branching units onto the free chain ends of the homogeneous Meyer structure, where two of these trifunctional groups bear the outer chains. Thus, the modified Meyer model has to be considered statistically as a copolymer. The procedure of calculation is essentially the same as for the homopolymer, with the difference that various tree structures have to be considered. Depending on the type of starting unit, these units are (i) a bifunctional repeating unit from an outer chain, (l_o), (ii) a trifunctional branching unit, (b_o), and (iii) a trifunctional repeating unit, (b_i), of the homogeneous Meyer model. The branching units b_i determine the size of the internal structure, while the b_o consists of one branching unit only. Here l_o defines the outer chain length, which in *all* models discussed remains the same. Accordingly, the population in the zeroth generation is a vector and in the first generation a matrix. The frequency of finding these different units furnishing the root of the various trees is given by the composition vector

$$\mathbf{m} = (m_{l_o}, m_{b_o}, m_{b_i}) \tag{A14}$$

where m_{l_o}, m_{b_o}, and m_{bi} are the mole fractions of these different units in the molecule. The corresponding equations for P_w, P_n, $P_z(q)$, and $\langle S^2\rangle_z$ are now given as follows:[5,33]

$$P_w = 1 + (\mathbf{m}[\langle \boldsymbol{N}(1)\rangle(\boldsymbol{I} - \boldsymbol{P})^{-1} \cdot \mathbf{1}]) \tag{A15}$$

$$P_n = 1/(1 - 0.5(\mathbf{m}[\langle \boldsymbol{N}(1)\rangle \cdot \mathbf{1}])) \tag{A16}$$

$$P_w P_z(q) = 1 + (\mathbf{m}[\langle \boldsymbol{N}(1)\rangle \tilde{\phi} \cdot (\boldsymbol{I} - \boldsymbol{P}\tilde{\phi})^{-1} \cdot \mathbf{1}]) \tag{A17}$$

$$\langle S^2\rangle_z = (b^2/2P_w)(\mathbf{m}[\langle \boldsymbol{N}(1)\rangle \cdot (\boldsymbol{I} - \boldsymbol{P})^{-2} \cdot \mathbf{1}]) \tag{A18}$$

where ϕ is given again by eq A10, with the only difference that b now is the average of three bond lengths.

Next we have to define the probabilities of reaction (link probabilities), from which the components of the population matrix in the first generation and of the transition probability matrix are derived. Let us define three types of units: I, unit from an outer chain; II, trifunctional coupling unit; and III, unit from the internal Meyer structure.

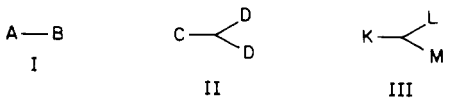

I II III

A, C, and K are terminal reducing groups. The various link probabilities are then given by Table IV. Some of these link probabilities have to fulfill the following constraints:

$$\alpha = \beta \tag{A19a}$$

$$\lambda = \mu = (1 - p)\varkappa + p\varkappa \tag{A19b}$$

$$\gamma = 1 \tag{A19c}$$

$$\delta = 1 \tag{A19d}$$

where p is the branching probability ($p = 0.04$), $\varkappa$ is the coupling probability via the reducing end groups. The last two conditions indicate that the branching unit is coupled with certainty onto a free end of the Meyer structure, and similarly, that the outer chains are coupled onto D groups. The population matrix $\langle \boldsymbol{N}(1) \rangle$ and the transition probability matrix $\boldsymbol{P}$ are then

$$\langle N(1) \rangle = \begin{array}{c} \\ l_o \\ b_o \\ b_i \end{array} \begin{array}{c} \begin{array}{ccccccc} A & B & C & D & K & L & M \end{array} \\ \begin{pmatrix} \beta & \alpha & 0 & 1-\alpha & 0 & 0 & 0 \\ 2 & 0 & 0 & 0 & 0 & 1 & 0 \\ 0 & 0 & 1-\lambda & 0 & \kappa & \lambda & \mu \end{pmatrix} \end{array} \tag{A20}$$

$$P = \begin{array}{c} \\ A \\ B \\ C \\ D \\ K \\ L \\ M \end{array} \begin{array}{c} \begin{array}{ccccccc} A & B & C & D & K & L & M \end{array} \\ \begin{bmatrix} \beta & 0 & 0 & 0 & 0 & 0 & 0 \\ 0 & \alpha & 0 & 1-\alpha & 0 & 0 & 0 \\ 2 & 0 & 0 & 0 & 0 & 0 & 0 \\ 1 & 0 & 0 & 0 & 0 & 1 & 0 \\ 0 & 0 & 1-\lambda & 0 & \kappa & 0 & 0 \\ 0 & 0 & 0 & 0 & \mu & \lambda & \mu \\ 0 & 0 & 1-\lambda & 0 & \lambda & \lambda & \mu \end{bmatrix} \end{array} \tag{A21}$$

Note: The difference between Table IV and the matrix $\boldsymbol{P}$ is that in the first case the *reaction* between two functionalities is considered, while in the other case the starting point is a backward-linked functionality. The *transition probability* represents then the various possibilities for reaching a special functionality in the next generation.

If we take into consideration the constraints of eq A19, it remains for us to define α, p, and $\varkappa$. The quantity α is defined by the outer chain length. Assuming a most probable distribution, one obtains

$$\bar{n}_o = 1/(1 - \alpha) \tag{A22}$$

which yields

$$\alpha = 0.926 \text{ for AP}$$

$$\alpha = 0.600 \text{ for } \beta\text{-LD}$$

The branching probability p of the cluster is

$$p_{\beta\text{-LD}} = 0.0714$$

which follows from the experimentally determined branching density for AP. The last probability, $\varkappa$, defines then the weight-average degree of polymerization.

In order to find the effective bond length, the degree of polymerization and the mean-square radius of gyration were calculated for various $\varkappa$ values, assuming an effective bond length of 1 nm. By this procedure one finds a curve that has to be compared with the point of measurements. The effective bond length is then obtained by adjusting the curve to the experimental point. The corresponding curves for the particle scattering factor are given in Figure 6. The small difference in the shape of the curves between AP and β-LD arises from the fact that the structure is not essentially changed when the outmost chains of the shell are removed, since the dimensions of the outer chains are small compared to $\langle S^2 \rangle_z$. The mass, however, is changed considerably because of the large number of outer chains.

Finally the mole fractions[4,35] m_{l_o}, m_{b_o}, and m_{b_i} of the composition vector have to be defined. These follow from the necessary condition that the total number of bonds from A-type units to units of type B must equal the number of bonds from B-type to A-type units. Furthermore the condition

$$\sum m_i = 1 \tag{A23}$$

is valid. This leads to the following relationships:

$$m_{l_o}(1 - \alpha) = m_{b_o}2 \tag{A24a}$$

$$m_{b_o} = m_{b_i}(1 - \lambda) \tag{A24b}$$

and with eq A23 one obtains

$$m_{b_i} = 1/[(1 - \lambda)(1 + (2/1 - \alpha))] \tag{A24c}$$

French Model. The list of link probabilities, given in Table V, and the elements of the matrices $\langle \boldsymbol{N}(1) \rangle$ and $\boldsymbol{P}$ are found for this model in the same manner, by inspection of Figure 12.

The elements of the matrices $\langle \boldsymbol{N}(1) \rangle$ and $\boldsymbol{P}$ are given in eq A25 and A26. (Note that inner and outer chains can both be coupled via E and D groups.) Again we have to assign special values for the link probabilities where the following equivalences are valid:

$$\alpha_1 = \beta_1 \tag{A27a}$$

$$\alpha_2 = \beta_2 \tag{A27b}$$

$$p = 1/2 \tag{A27c}$$

$$\epsilon = \delta = \gamma/2 \tag{A27d}$$

The value $p = 1/2$ corresponds to a 50% branching density of the clusters.[38] It therefore remains to assign values for α_1, α_2, γ, r, and $\varkappa$.

The quantity α_1 is determined by the length of the inner chain, i.e., $\bar{n}_{i2} = 1/(1 - \alpha_1) = 22$, from which follows $\alpha_1 = 21/22$. The outer chains are the same as in the Meyer model, i.e., $\alpha_2 = 0.926$ for AP and $\alpha_2 = 0.60$ for β-LD. The

$$\langle N(1) \rangle = \begin{array}{c} \\ m_{l_i} \\ m_{l_o} \\ m_b \end{array} \begin{array}{c} \begin{array}{ccccccc} A_1 & B_1 & A_2 & B_2 & C & D & E \end{array} \\ \begin{pmatrix} \beta_1 & \alpha_1 & 0 & 0 & (1-\beta_1)\kappa & (1-\alpha_1)/2 & (1-\alpha_1)/2 \\ 0 & 0 & \beta_2 & \alpha_2 & 0 & (1-\alpha_2)/2 & (1-\alpha_2)/2 \\ r(2-\gamma)/2 & (1-\gamma)\kappa & (1-r)(2-\gamma)/2 & 0 & \gamma & (1-p)\gamma & p\gamma \end{pmatrix} \end{array} \tag{A25}$$

$$P = \begin{array}{c} \\ A_1 \\ B_1 \\ A_2 \\ B_2 \\ C \\ D \\ E \end{array} \begin{array}{c} \begin{array}{ccccccc} A_1 & B_1 & A_2 & B_2 & C & D & E \end{array} \\ \begin{bmatrix} \beta_1 & 0 & 0 & 0 & (1-\beta_1)\kappa & 0 & 0 \\ 0 & \alpha_1 & 0 & 0 & 0 & (1-\alpha_1)/2 & (1-\alpha_1)/2 \\ 0 & 0 & \beta_2 & 0 & 0 & 0 & 0 \\ 0 & 0 & 0 & \alpha_2 & 0 & (1-\alpha_2)/2 & (1-\alpha_2)/2 \\ r(2-\gamma)/2 & 0 & (1-r)(2-\gamma)/2 & 0 & \gamma & 0 & 0 \\ r(1-\epsilon)/2 & (1-\gamma)\kappa & (1-r)(1-\epsilon) & 0 & \epsilon & \delta & \epsilon \\ r(1-\delta)/2 & (1-\gamma)\kappa & (1-r)(1-\delta)/2 & 0 & \delta & \delta & \epsilon \end{bmatrix} \end{array} \tag{A26}$$

$$\langle N(1)\rangle = \begin{array}{c} \\ m_i \\ m_o \\ m_b \\ m_{b_i} \end{array} \begin{array}{c} \begin{array}{ccccccccccc} A_1 & B_1 & A_2 & B_2 & C & D & E & R & S & T \end{array} \\ \begin{pmatrix} \alpha_1 & \beta_1 & 0 & 0 & 0 & (1-\alpha_1)/4 & (1-\alpha_1)/4 & (1-\beta_1) & (1-\alpha_1)/2 & 0 \\ 0 & 0 & \alpha_2 & \beta_2 & 0 & (1-\alpha_2)/2 & (1-\alpha_2)/2 & 0 & 0 & 0 \\ (2-\gamma)/2 & 0 & (1-r)(2-\gamma)/2 & 0 & \gamma & \delta & \epsilon & 0 & 0 & (1-\gamma)\kappa \\ \sigma & 1 & 0 & 0 & \tau & 0 & 0 & 0 & 0 & 0 \end{pmatrix} \end{array} \tag{A31}$$

$$P = \begin{array}{c} \\ A_1 \\ B_1 \\ A_2 \\ B_2 \\ C \\ D \\ E \\ R \\ S \\ T \end{array} \begin{array}{c} \begin{array}{ccccccccccc} & m_i & & m_o & & & m_b & & & m_{bi} & \\ A_1 & B_1 & A_2 & B_2 & C & D & E & R & S & T \end{array} \\ \begin{pmatrix} \alpha_1 & 0 & 0 & 0 & 0 & 0 & 0 & (1-\alpha_1) & 0 & 0 \\ 0 & \alpha_1 & 0 & 0 & 0 & (1-\alpha_1)/4 & (1-\alpha_1)/4 & 0 & (1-\alpha_1)/2 & 0 \\ 0 & 0 & \alpha_2 & 0 & 0 & 0 & 0 & 0 & 0 & 0 \\ 0 & 0 & 0 & \alpha_2 & 0 & (1-\alpha_2)/2 & (1-\alpha_2)/2 & 0 & 0 & 0 \\ r(2-\gamma)/2 & 0 & (1-r)(2-\gamma)/2 & 0 & \gamma & 0 & 0 & 0 & 0 & 0 \\ r(1-\epsilon)/2 & 0 & (1-r)(1-\gamma)/2 & 0 & \epsilon & \delta & \epsilon & 0 & 0 & (1-\gamma)\kappa \\ r(1-\delta)/2 & 0 & (1-r)(1-\gamma)/2 & 0 & \delta & \delta & \epsilon & 0 & 0 & (1-\gamma)\kappa \\ \sigma & 0 & 0 & 0 & \tau & 0 & 0 & 0 & 0 & 0 \\ 0 & 1 & 0 & 0 & \tau & 0 & 0 & 0 & 0 & 0 \\ \sigma & 1 & 0 & 0 & 0 & 0 & 0 & 0 & 0 & 0 \end{pmatrix} \end{array} \tag{A32}$$

number-average degree of polymerization of the cluster P_{nc} is determined, on one hand, by eq A16, and on the other, by eq 2

$$P_n = Z_k/DB = 3.2/0.5 = 6.4 \tag{A28}$$

where $Z_k = 3.22$ of Table II was used. This yields

$$\gamma = 5.4/6.4$$

The ratio r of the inner and outer chains coupled onto the free end groups of the clusters is

$$r = 1/4.22$$

The coupling probability κ (via the reducing end groups C; see Figure 12) is found by variation until the calculated M_w agrees with the experimental value. To find the effective bond length we proceed in the same manner as described for the Meyer model.

The mole fractions m_{l_o}, m_b, and m_{l_i} are calculated as outlined for the Meyer model, which gives eq A29

$$m_{l_o}(1-\alpha_2) = m_b((1-r)(2-\gamma)/2) \tag{A29a}$$

$$m_{l_i}2(1-\alpha_A) = m_b(r(2-\gamma)/2 + (1-\gamma)\kappa) \tag{A29b}$$

With eq A23 and A29 one obtains the mole fractions

$$m_{l_i} = m_b(0.5r(2-\gamma) + (1-\gamma)\kappa)/(1+\kappa)(1-\alpha_1) \tag{A30a}$$

$$m_{l_o} = m_b(0.5(1-r)(2-\gamma))/(1-\alpha_2) \tag{A30b}$$

$$m_b = [1 + (0.5(1-r)(2-\gamma)/(1-\alpha_2)) + (0.5r(2-\gamma) + (1-\gamma)\kappa)/(1+\kappa)(1-\alpha_1)]^{-1} \tag{A30c}$$

When κ has been found from M_w, no other fitting parameter is left and $P_z(q)$ is uniquely defined.

Modified Robin–Mercier Model. For the modified Robin–Mercier model one can derive the list of link probabilities (Table VI) and the elements of the matrices $\langle \boldsymbol{N}(1)\rangle$ and $\boldsymbol{P}$ as outlined for the other models (see Figure 13).

The elements for the matrices $\langle \boldsymbol{N}(1)\rangle$ and $\boldsymbol{P}$ are given in eq A31 and A32, where we assumed that the free end groups A_1 can react with the same probability with the functional group (E and D) and S. The values for the probabilities α_1, α_2, γ, and $\epsilon = \delta = \gamma/2$ are the same as for the French model. The value for the probability σ is determined by the number of coupled internal chains $\bar{n}$.

$$\bar{n} = 1/(1-\sigma) \tag{A33}$$

There remains the assignment of the values to the probabilities τ and κ and the molar ratio of the various types of monomers. These ratios are derived as before from the balance of bonds, which leads to

$$0.5m_i(1-\alpha_1) = m_b(r/2)(2-\gamma) \tag{A34a}$$

$$m_o(1-\alpha_2) = 0.5m_b(1-r)(2-\gamma) \tag{A34b}$$

$$m_b(1-\gamma)\kappa = m_{b_i}\tau \tag{A34c}$$

$$m_i(3/2)(1-\alpha_1) = m_{bi}(1+\sigma) \tag{A34d}$$

The system of equations is overdetermined and thus leads to a correlation between the probability κ and τ as given by

$$\tau = (1/3)(1+\sigma)(1-\gamma)(r(2-\gamma))^{-1}\kappa \tag{A35}$$

For the mole fractions of the components we obtain

$$m_{b_i} = (1 + (2/3)(1+\sigma)(1-\alpha_1))^{-1}[1 + r(2-\gamma) \times (1-\alpha_1)^{-1} + (1-r)(2-\gamma)(2(1-\alpha_2))^{-1}]^{-1} \tag{A36a}$$

and

$$m_b = (2/3)(1+\sigma)(1-\alpha_1)^{-1}m_{b_i} \tag{A36b}$$

$$m_o = (1-r)(2-\gamma)(1-\alpha_2)m_b \tag{A36c}$$

$$m_i = 2r(2-\gamma)(1-\alpha_1)m_b \tag{A36d}$$

Again as in the other models, the coupling parameter of the reducing end κ was varied until the correct M_w was obtained. The only parameter left to be evaluated is the average number $\bar{n}$ defining the length of the side chain, and this was found by the fit of the angular dependence of $P_z(q)$.

Registry No. AP, 9037-22-3.

References and Notes

(1) Stockmayer, W. H. *J. Chem. Phys.* **1943**, *11*, 45; **1944**, *12*, 125.
(2) Zimm, B. H.; Stockmayer, W. H. *J. Chem. Phys.* **1949**, *17*, 1301.
(3) Flory, P. J. "Principles of Polymer Chemistry"; Cornell University Press: Ithaca, NY, 1953.
(4) Gordon, M. *Proc. R. Soc. London, A* **1962**, *268*, 240.
(5) Burchard, W. *Adv. Polym. Sci.* **1983**, *48*, 1.
(6) Bantle, S. Ph.D. Thesis 1982, Freiburg.
(7) Gordon, M.; Parker, T. G. *Proc. R. Soc. Edinburgh, Sect. A: Math. Phys. Sci.* **1971**, *69*, 13.
(8) Dušek, K. *Makromol. Chem. Suppl.* **1979**, *2*, 35.
(9) Meyer, K. H.; Bernfeld, P. *Helv. Chim. Acta* **1940**, *23*, 865.
(10) French, D. *Denpun Kagaku* **1972**, *19*, 8.
(11) Kainuma, K.; French, D. *Biopolymers* **1971**, *10*, 1673.
(12) Kainuma, K.; French, D. *Biopolymers* **1972**, *11*, 2241.
(13) Gunja-Smith, Z.; Marshall, J. J.; Mercier, C.; Smith, E. E.; Whelan, W. J. *FEBS Lett.* **1970**, *12*, 101.
(14) Lee, E. Y. C. *Arch. Biochem. Biophys.* **1971**, *146*, 488.
(15) Lee, E. Y. C.; Whelan, W. J. *Enzymes* **1971**, *5*, 191.
(16) Robin, J. P.; Mercier, C.; Duprat, F.; Charbonniere, R.; Guilbot, A. *Starch/Staerke* **1975**, *27*, 36.
(17) Robin, J. P.; Mercier, C.; Charbonniere, R.; Guilbot, A. *Cereal Chem.* **1974**, *51*, 389.

(18) Burchard, W.; *Macromolecules* **1972**, *5*, 604.
(19) Burchard, W.; Eschwey, A.; Franken, I.; Pfannemüller, B. In "Structure of Fibrous Biopolymers"; Butterworth: London, 1975.
(20) Erlander, S. R.; French, D. *J. Polym. Sci.* **1956**, *20*, 7.
(21) Thurn, A.; Burchard, W.; Proc. Sympos. "Plant Polysaccharides" p. 31, 1984.
(22) Bathgate, G. N.; Manners, D. J. *Biochem. J.* **1966**, *101*, 30.
(23) Manners, D. J.; Matheson, N. K.; *Carbohyd. Res.* **1981**, *90*, 99.
(24) Staudinger, H.; Husemann, E. *Justus Liebigs Ann. Chem.* **1937**, *527*, 195.
(25) Harworth, W. N.; Hirst, E. L.; Isherwood, F. A. *J. Chem. Soc.* **1977**, 577.
(26) Greenwood, C. T.; Milne, E. A. *Adv. Carbohyd. Chem.* **1968**, *23*, 281.
(27) Banks, W.; Greenwood, C. T. "Starch and its Components"; Edinburgh University Press: Edinburgh, 1975.
(28) Heyns, K. "Die neueren Ergebnisse der Staerkeforschung"; Vieweg: Braunschweig, 1949.
(29) Flory, P. J. *J. Am. Chem. Soc.* **1941**, *63*, 3083, 3091, 3096.
(30) Burchard, W.; Bantle, S.; Müller, M.; Reiner, A. *Pure Appl. Chem.* **1981**, *53*, 1519.
(31) Kajiwara, K.; Burchard, W.; Gordon, M.; *Br. Polym. J.* **1970**, *2*, 110.
(32) Kajiwara, K. *Polymer* **1971**, *12*, 57.
(33) Gordon, M.; Malcolm, G. N.; Butler, D. S. *Proc. R. Soc. London A* **1966**, *295*, 29.
(34) Dobson, G. R.; Gordon, M. *J. Chem. Phys.* **1964**, *41*, 2389.
(35) Gordon, M. "Colloquia Mathematica Societatis Janos Bolyai"; North Holland: Amsterdam, 1970; p 511.
(36) Eschwey, A.; Burchard, W.; Pfannemüller, B., unpublished data, manuscript in preparation.
(37) Actually $Z_k + 1$ is the number of outer chains; the chains connecting two clusters are also outer chains that became longer chains by coupling two clusters. In the β-LD only the free-ended outer chains can be attacked by β-amylase.
(38) The cluster has been calculated according to the AB_2 model (see Figure 3b), where A can react with B only. Then P_w is given[5,40] as $P_w = 1 - \alpha^2[(1-p)^2 + p^2]/(1-\alpha)^2$, where p is the branching probability and $\bar{n}_{ic} = 1/p$. Evidently the highest branching probability is 0.5 and yields $\bar{n}_{ic} = 2$.
(39) Note: There are three types of internal chain length: $\bar{n}_{ic}$ = a chain connecting two branching points in a cluster; $\bar{n}_{i2}$ = chain length connecting two clusters; $\bar{n}_{is}$ = length of a side chain, emerging from one cluster, carrying on the average $\bar{n}$ clusters.
(40) Burchard, W. *Macromolecules* **1977**, *10*, 919.

Notes

On the Excluded Volume Perturbation

HIDEMATSU SUZUKI

Institute for Chemical Research, Kyoto University, Uji, Kyoto-fu 611, Japan. *Received November 26, 1984*

It is a significant contribution that Muthukumar and Nickel recently evaluated the fourth to sixth coefficients, for the first time, in the excluded volume perturbation expansion of $\langle R^2 \rangle$ (the mean-square end-to-end distance) in three dimensions:[1]

$$\alpha_R{}^2 \equiv \langle R^2 \rangle / \langle R^2 \rangle_0 = 1 + \sum_{i=1}^{\infty} C_i z^i \qquad (1)$$

Here, $\alpha_R{}^2$ is the square expansion factor defined by the ratio $\langle R^2 \rangle / \langle R^2 \rangle_0$, the subscript 0 refers to the unperturbed state, C_i is the numerical coefficient, and z stands for the (conventional) excluded volume variable.[2] The values of C_1 to C_6 obtained by them are reproduced in the second column of Table I.[3] Eighteen years ago, Yamakawa and Tanaka calculated the third coefficient as 6.459,[4] while Muthukumar and Nickel now give 6.296... to C_3.[5] They claim that the result of Yamakawa and Tanaka is in error but do not even mention a few, more important points in their paper.

The first point concerns the divergence of the series, eq 1, clearly suggested by their numerical figures for C_i's. Fixman[2] and Yamakawa[6] stated, without proof, that the series very slowly converges, but that does not seem to be true. Serious doubt about the convergence has already been cast by several authors.[7-11] The recent results of Muthukumar and Nickel support the latter view on the (conventional) perturbation expansion.

Table I
Numerical Comparison of the Perturbation Coefficients in Eq 1

C_i	Muthukumar–Nickel[1]	eq 2[a]
C_1	$^4/_3$	1.333
C_2	−2.075 385 396	−2.075
C_3	6.296 879 676	6.459
C_4	−25.057 250 72	−25.13
C_5	116.134 785	109.5
C_6	−594.716 63	−511.2

[a] Coefficients were obtained by expanding eq 2 into a series.

The second point is that the approximate value −25.3 for C_4 given by Gordon et al.[8] is in good agreement with −25.057.... The third point concerns the comparison between the results of Muthukumar and Nickel and the coefficients obtained by expanding the following closed-form expression for $\alpha_R{}^2$:

$$\alpha_R{}^2 = 0.5716 + 0.4284(1 + 6.225z)^{1/2} \qquad (2)$$

This expression has been published in a form with three significant figures by Yamakawa and Tanaka[4] and Suzuki.[12] Equation 2 is known to be valid at least up to third-order perturbation theory.[12] The first six coefficients obtained by expanding eq 2 are listed in the third column of Table I. From this table, one can see good agreements between the two series of numerical figures. Even for the sixth coefficient, the value from eq 2 differs only by 14% from that of Muthukumar and Nickel. Thus, a simple closed-form expression, eq 2, finds theoretical support from their higher order perturbation calculation. Other expressions also can be assessed by similar comparison.[13]

0024-9297/85/2218-2082$01.50/0